Real-Time Optical Monitoring of Epitaxial Growth: Pulsed Chemical Beam Epitaxy of GaP and InP Homoepitaxy and Heteroepitaxy on Si

N. DIETZ,[†*] U. ROSSOW,[†] D. ASPNES,[†] and K.J. BACHMANN[*‡]

Department of Materials Science and Engineering,[*] Department of Physics,[†] and Department of Chemical Engineering,[‡] North Carolina State University, Raleigh NC 27695-7919

We present a study of the real-time monitoring of the homoepitaxial growth of GaP, InP, and the growth of InP/GaP and GaP/Si(001) heterostructures, combining single wavelength p-polarized reflectance (PRS), reflectance-difference spectroscopy (RDS), and laser light scattering (LLS) during pulsed chemical beam epitaxy with tertiarybutylphosphine, triethylgallium, and trimethylindium sources. The growth rate and the bulk optical properties are revealed by PRS with submonolayer resolution over 1000Å of film growth. The surface topography is monitored by LLS providing additional information on the evolution of the surface roughness as well as the nucleation/growth mechanism. The optical surface anisotropy, which is related to surface reconstruction and/or surface morphology, is monitored by RDS and compared with the results of PRS and LLS. The results are discussed with respect to the deposition kinetics, in particular as a function of the V:III flux ratio. The pulsed supply of chemical precursors causes a periodic alteration of the surface composition, which is observed as correlated periodic changes in the RD and PR signals, confirming the high sensitivity of both methods to surface chemistry.

Key words: GaP, InP, pulsed chemical beam epitaxy (PCBE), real-time monitoring

INTRODUCTION

The real-time monitoring of epitaxial growth by nonintrusive methods is important for meeting the increasingly stringent tolerances of complex device structures as well as for achieving a better understanding of growth mechanisms in the engineering of epitaxial layers with well defined optical and electrical properties. Surface-sensitive methods such as reflection high energy electron diffraction (RHEED),[1] reflectance-difference spectroscopy (RDS),[2] surface photo absorption (SPA),[3–5] and laser light scattering (LLS)[6] are providing new insights into surface chemistry and morphology during growth. The high sensitivity of these methods to surface/interface phenomena independent of bulk optical properties and film thicknesses limits their applicability to real-time control. Optical techniques such as kinetic reflectometry at both single[7] and multiple[8] wavelengths, pyrometric interferometry (PI)[9] and spectral ellipsometry (SE) can be used to monitor bulk-related properties and in at least one case have been used successfully for close-loop feedback control of epitaxy.[10] However, reflectance changes due to chemical modifications of the surface are of the order of 10^{-3} to 10^{-4} and are difficult to detect in normal incidence reflectance measurements.

In order to increase the sensitivity to surface and interface related growth properties, we recently introduced a new optical technique, p-polarized reflectance (PRS), which not only achieves high sensitivity to surface chemistry but also probes bulk material and buried interfaces and can be applied to control film thickness with sub-monolayer resolution.[11–14]

(Received April 4, 1995)

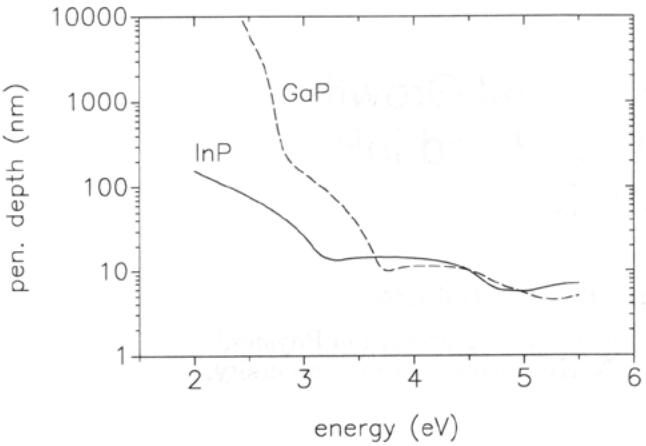

Fig. 1. Spectral dependence of the penetration depth of light in GaP and InP.

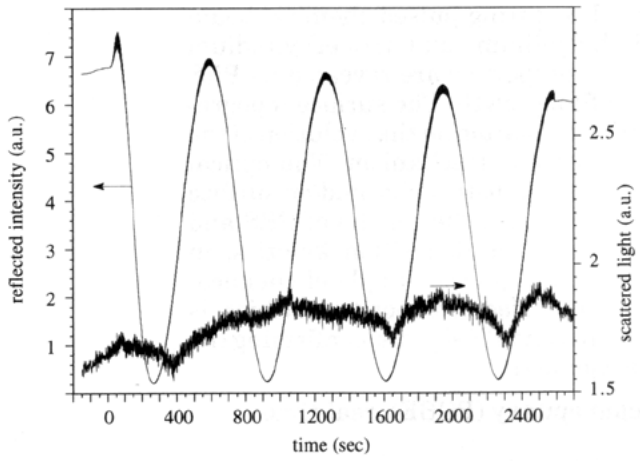

Fig. 2. P-polarized reflectance signal (upper curve) and scattered light intensity (lower curve) for heteroepitaxial film growth of GaP on Si(001) at 350°C with a 3 s cycle sequence time.

However, to separate the various effects contributing to PRS, correlations with other ex-situ and in-situ measurements are essential. These correlations are also expected to provide a better understanding of growth kinetics and better identification of information that may be useful for process control.

In this paper, we describe the simultaneous application of PRS, RDS, and LLS for monitoring heteroepitaxial film growth of InP on GaP substrates and GaP on Si substrates as well as the homoepitaxial growth of GaP and InP epilayers. The surface-sensitive probes respond to changes of surface reconstructions and morphologies, which are important in heteroepitaxial nucleation and growth on silicon and which must be followed carefully to avoid the formation of defects associated with lattice strain and chemical incompatibilities in the nucleation and early stages of heteroepitaxial growth.[13] The combined application of PRS, RDS, and LLS for real-time probing of surface, interface and bulk properties provides insight into the kinetics and mechanisms of deposition processes and allows us to evaluate and improve process conditions, such as surface preconditioning, deposition temperature, and V-III precursor ratio, for the preparation of improved materials.

EXPERIMENT

For PRS and LLS, we employed a p-polarized beam generated by a HeNe laser ($\lambda = 632.8$ nm) and a Glan-Thompson prizm. The beam was incident at $\varphi \approx 72° \pm 3°$ near the Brewster angles of the substrates. The reflected beam is detected by a Si photodiode with a integrated preamplifier, the output of which is processed by a lock-in amplifier and recorded by a data acquisition system. The scattered radiation is detected simultaneously by a photomultiplier tube (PMT) located 45° away from the plane of incidence.

Reflectance-difference spectrsocopy measures the optical anisotropy of the sample, which is normally dominated by that between the [$\bar{1}$10] and [110] principal axes of the (001) surface. The configuration and approach have been described in detail elsewhere.[15] The spectral range is 1.5 to 5.5 eV. The light enters the chamber through a nominally strain-free quartz window.[16] Residual strain effects were corrected by subtracting a baseline spectrum that was obtained on a sample that exhibits no anisotropy. For the materials of interest here, the penetration depths of light depends on photon energy as shown in Fig. 1. For GaP, homoepitaxy contributions from the back side of the substrate to the RDS spectra cannot be excluded in the energy range below 2.5 eV. Therefore, these specta are presented only above 2.5 eV.

The fluxes of the precursors triethylgallium [TEG, $Ga(C_2H_5)_3$], tertiarybutyl phosphine [TBP, $(C_4H_9)PH_2$], trimethylindium [TMIn, $In(CH_3)_3$], and hydrogen, are established by mass flow controllers and are directed via computer-controlled three-way valves to either the reactor chamber or a separately pumped bypass chamber.[11,13,17] This allows the sequential exposure of the substrate to individual pulses of the precursor molecules. The total gas flow during deposition leads to a pressure in the low 10^{-4} mbar range. The switching of the sources is synchronized with the data acquisition of the PRS and LLS signals to relate observed changes in the reflected intensity of the light to chemistry-induced changes in the optical properties. The Si(001) substrates, vicinally cut 4° toward (111) [arsenic-doped 1–25 Ωcm], 6° toward (011) [boron-doped 1–10 Ωcm], and 10° toward (011) [arsenic-doped 6–12 Ω cm] were given an RCA clean followed by a DI-H_2O rinse, a final buffered HF dip and a short DI-H_2O rinse before being transferred via a load-lock into the growth chamber. This treatment produces a (1 × 1) hydrogen terminated Si (001) surface as verified by RHEED. The on-axis sulfur-doped (2×10^{17} cm^{-3}) GaP(001) substrates were ex-situ cleaned using a Br-methanol rinse, followed by a DI-H_2O rinse, a NH_4OH:H_2O (2:5) dip for 2 min and a final DI-H_2O rinse. For InP homoepitaxy, Zn-doped (6×10^{18} cm^{-3}) InP(001) substrates were used after being preconditioned as GaP. Before epitaxial growth was initiated, the GaP and InP substrates are raised to elevated temperatures under a continuous flow of TBP to desorb the oxides.[18]

RESULTS

GaP Heteroepitaxy on Si

Upon initiating heteroepitaxial growth, the PRS signal oscillates with a period corresponding to quarter wavelength film thickness as illustrated in Fig. 2 for GaP heteroepitaxy on a 4° vicinal p-Si (001) substrate at 380°C. The reflected intensity increases during heating to the growth temperature due to the changes in the dielectric function of the substrate. It is also strongly affected by surface preconditioning. Appropriate preconditioning results in a stabilized reflected intensity after the growth temperature has been reached. A flux of filament activated Pd-purified hydrogen is provided continuously.

Growth is done using sequential pulses of TPB and TEG separated by delays. Typical durations are 1.5 s of TBP, a 0.6 s delay, 0.3 s of TEG, and a 0.6 s delay, as illustrated schematically in Fig. 3. The flux intensity of TBP and TEG for Fig. 2 is 0.8 and 0.02 sccm, respectively, resulting in a total V-III flux ratio of 200:1. For this condition, the growth rate per cycle sequence is estimated to be 3.6Å/cycle assuming a constant growth rate over the entire deposition process. Also shown in Fig. 2 (lower curve) is the intensity of the scattered light as a function of the growth time. The diffuse scattering signal increases slightly during the 4000Å of film growth with well-pronounced features during the film growth. These features also contribute to the final roughening of the surface as observed ex-situ by AFM.[14]

These sequential exposures generate a fine structure that is superimposed on the quarter-wavelength oscillations. This fine structure is maintained throughout the entire film growth with a periodicity strongly related to a complete pulse cycle sequence. This fine structure is shown in detail in Figs. 4a through 4c for three different sets of conditions: (a) 3 s cycle time with 1.5 s of TBP, a 0.6 s delay, 0.3 s of TEG, and a 0.6 s delay; (b) 4 s cycle time with 0.8 s of TBP, a 1.2 s delay, 0.2 s of TEG, and a 0.8 s delay, and (c) 7 s cycle time with 0.8 s of TBP, a 3.2 s delay, 0.2 s of TEG, and a 2.8 s delay. The flux intensities of TBP and TEG of 0.8 and 0.02 sccm, respectively, are kept constant. Under this growth condition, the growth rate per cycle can vary from 1 to 3.6Å per cycle, where an asymptotic saturation seems to be reached.[11]

Figure 4 also shows that the fine-structure exhibits a strong periodic modulation of its envelope by nearly a factor of two. This envelope modulation occurs even though the pulse sequence is kept invariant, which indicates that the fine structure does not depend only on the pulse sequence, but also on periodic changes of surface conditions on a longer time scale. Note that the modulation of the amplitude and baseline exhibits at least two frequencies. The detailed appearance depends strongly on the chosen individual precursor exposure durations. Conditions exist for which the envelope is smooth (curve a) or exhibits a bimodal behavior (curves b and c).

Figure 5a shows the changes in the PRS and LLS signals during the epitaxial growth of a GaP epilayer on a 10° vicinal Si(001) wafer. Here the growth rate is significantly reduced by placing an orifice over the TEG outlet. The increase in the PRS signal in the first few minutes is due to heating the sample to 600°C during which a pulsed TBP flux is applied. After 2 min at 600°C, the temperature is lowered to 350°C, where epitaxial growth of GaP takes place after the PRS signal is stabilized (t = 400 s). When growth begins, the PRS signal shows an increased first maximum

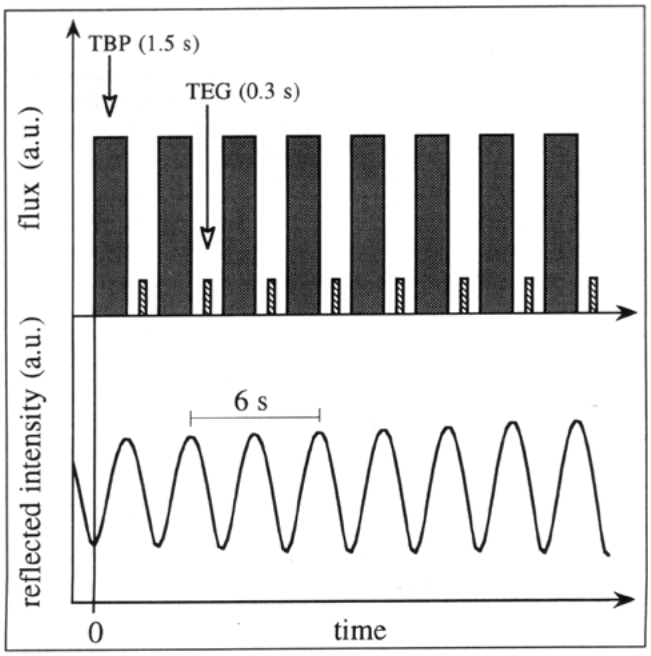

Fig. 3. TBP and TEG pulse sequence (top) with the corresponding oscillation in the PRS signal for a 3 s cycle sequence time.

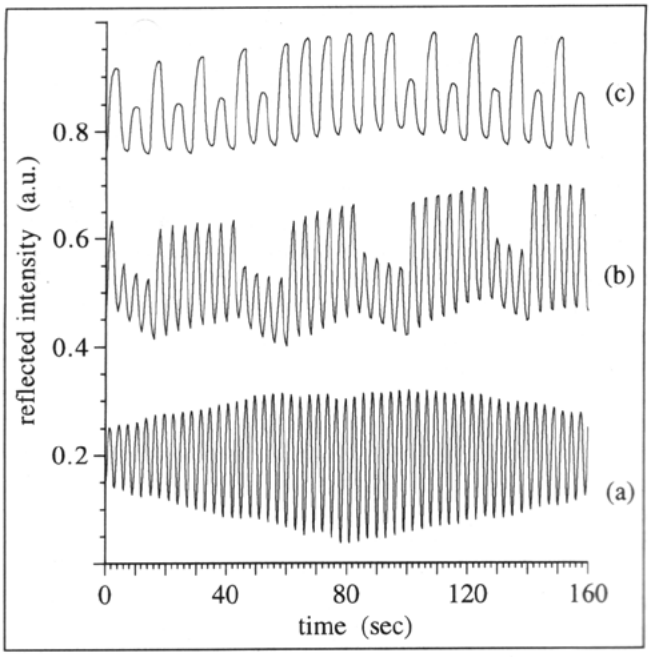

Fig. 4. Variation in the amplitude modulated fine structure in the PRS-signal for (a) 3 s, (b) 4 s, and (c) 7 s cycle sequence time for heteroepitaxial growth of GaP on Si(001) at 310°C.

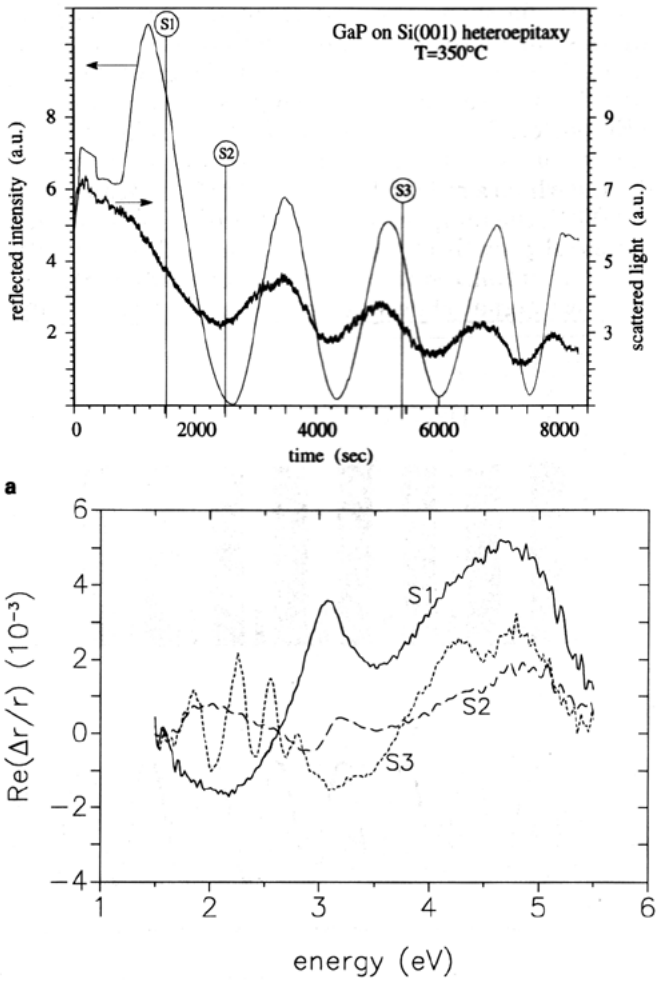

Fig. 5. (a) P-polarized reflectance signal (upper curve) and scattered light intensity (lower curve) for heteroepitaxial film growth of GaP on Si(001) (10° off-cut) at 350°C with a 3 s cycle sequence time, and (b) time evolution of the anisotropy of the RDS-signal at selected points S1, S2, and S3 as marked in Fig. 5 (a). These spectra are digital filtered.

before starting to oscillate with the quarter-wavelength pattern exhibited during prolonged film growth. Note, that the diffuse scattered intensity of the Si substrate is strongly increased compared to that of the 4° vicinal substrate (see Fig. 2) or to an on-axis Si-substrate (not shown). This could be related to a large number of steps on the surface. During film growth, the diffuse scattered intensity shows pronounced oscillations, which differ from the observed quarter-wavelength oscillation in the reflected intensity. However, the overall scattered intensity is significantly reduced, suggesting a smoothening of the surface topography. At present, it is not clear to which degree the changes in the scattered light are related to changes in the surface morphology or the heteroepitaxial interface.

Reflectance-difference spectra taken during deposition are shown in Fig. 5b for selected points during the growth process as labeled in Fig. 5a. For the S3, spectrum obtained at the highest coverage interference fringes are seen below 3eV, where the penetration depth of light is still much higher than the layer

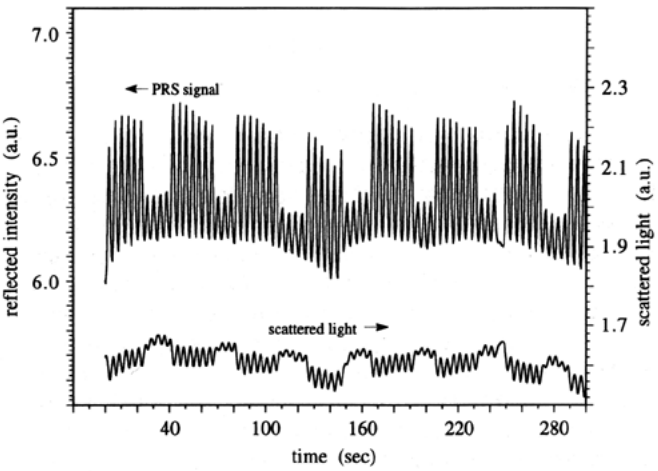

Fig. 6. Changes in the amplitude modulated fine structure of the PRS signal and correlated changes in the intensity of the scattered radiation during the homoepitaxial growth of GaP on vicinal GaP(001) at 310°C.

thickness. For the S1 spectrum obtained at lowest coverage, a 3.1 eV feature appearing that GaP homoepitaxy occurs (see Fig. 9b). This feature vanishes with increasing layer thickness. For reasons that are not clear at higher energies, a broad feature near 4.7 eV becomes resolved with increasing thickness into a doublet. A similar double feature is observed for double-domain vicinal silicon (001)-wafers and probably originates from step structure of the surface.[19,20] Hence, we believe that for GaP, which is nearly lattice matched to silicon, this double feature is also related to the steps on the surface. This step structure should be better defined as the surface becomes smoother with increasing thickness, and is accompanied by a decrease of the scattered light as also seen in Fig. 5a.

GaP and InP Homoepitaxy

Under homoepitaxial growth, the quarter-wavelength PRS oscillation vanishes due to the absence of interference generated by the differences in the dielectric functions of film and substrate. However, in the homoepitaxial growth of InP and GaP, the envelope modulation of the fine structure remains, with the same periodicity as observed under heteroepitaxial growth conditions. Figure 6 shows an example of these oscillations in the PRS-signal and the corresponding changes in the intensity of the scattered light during GaP homoepitaxy at 310°C with a cycle time of 4 s. For InP homoepitaxy, the scale of the oscillations is not as well pronounced as for GaP, which could be due to the different values of the pseudo-Brewster angle [φ_B(InP) ≈ 74.5° and φ_B(GaP) ≈ 72.5° at λ = 632.8 nm].

Under the observed homoepitaxial conditions, the LLS intensity shows a modulated fine structure of opposite sign with respect to the PRS signal, which also follows following the periodicity of the precursor cycle sequence. This correlation is not observed for heteroepitaxial growth on Si. During homoepitaxial growth of InP and GaP, similar growth oscillation have been observed in selected energy ranges of the

RDS spectra. Figure 7 shows these oscillations as they occur during the growth of InP and GaP homoepitaxy and InP-GaP heteroepitaxy. These oscillations can be related to periodic changes of the surface reconstruction caused by the successive changes in the surface composition upon exposure to t-butPH_2 and trimethylindium, respectively.

Figure 8a shows the changes that occur in the PRS and LLS signals during InP homoepitaxy when conditions are changed in a stepwise manner from phosphorus-rich to indium-rich. The times when changes occur are marked I1 through I5. These produce related changes in RDS spectra as shown in Figs. 8b and 8c. Here growth is begun under phosphorus-rich conditions with TBP:TMIn = 400: 1 (→RDS spectrum I1 and I2) and increased to TBP:TMIn = 200:1 at t = 5100 s (→RDS spectrum I3), followed by TBP:TMIn = 60:1 at t = 8200 s (→RDS spectrum I4), and TBP:TMIn = 40:1 at t = 9200 s (→RDS spectrum I5). The fluctuations in the PRS signal occurring over a time range of 5 to 10 min are also observable in LLS indicating periodic changes in the surface morphology. However, the overall LLS intensity does not increase. With a TBP:TMIn ratio ≤60:1, the LLS intensity increases steadily indicating a significant enhancement of the surface roughness.

The overall line-shape of the RDS spectra taken during InP homoepitaxy is in good agreement with published data.[21] These spectra show a deep minimum near 1.9 eV and three maxima at higher energies (2.6, 3.5, and 4.2 eV), which could not be attributed to electronic transitions in the surface region. To determine the influence of the surface chemical composition, the In flux was varied while the TBP flux was held at a constant high value. A significant lineshape is observed (see Fig. 8b). While the minimum is not affected, all maxima change. The dominant effect is that the edge approaching the second maximum near 3 eV becomes weaker with increasing In flux. This effect can be seen better in Fig. 8c where the differences relative to the spectrum I1 are shown. The signal-to-noise ratio is enhanced by Fourier filtering. In Fig.8b, two spectral regions, marked by arrows, exhibit growth oscillations. The signal variation in these regions is due to these oscillations and not to noise. One such transient is shown in Fig. 7. Note that the amplitude of the anisotropy oscillation in InP homoepitaxy is as large as that during GaP homoepitaxy.

Heteroepitaxy InP on GaP

Figure 9a shows the evolution of the PRS signal and LLS intensity during GaP homoepitaxy followed by InP heteroepitaxy on a GaP substrate. During GaP homoepitaxy, the PRS signal and LLS intensity show long-term oscillations of the order of 200–300 s related to small periodic changes in surface morphology. The overall scattered light intensity remains stable. After depositing several 100 nm of GaP growth is switched to InP. The PRS signal starts to increase and evolves into quarter-wavelength oscillations after prolonged periods. The LLS intensity decreases slightly and stays nearly constant during further growth. The RDS spectra just before and after this transition are shown in Fig. 9b. The spectrum at G1 is similar to that observed for InP, except that a double feature is observed near 3.2 eV. Immediately after switching, this feature changes to a single peak

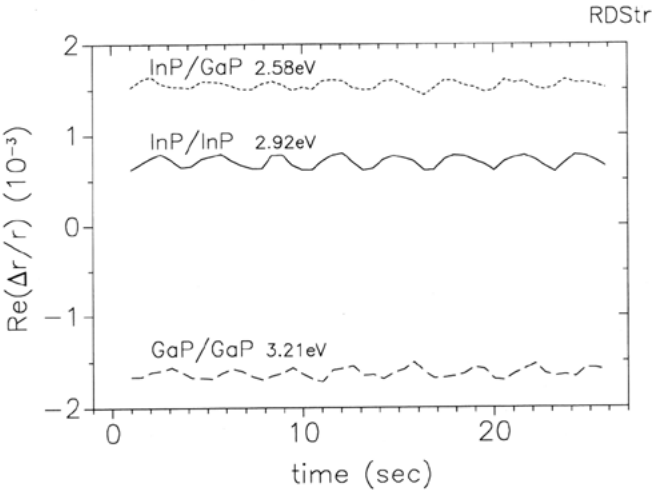

Fig. 7. Alternating changes in the anisotropy of the surface at selected energies as they can be observed in the RDS signal under the condition of PCBE.

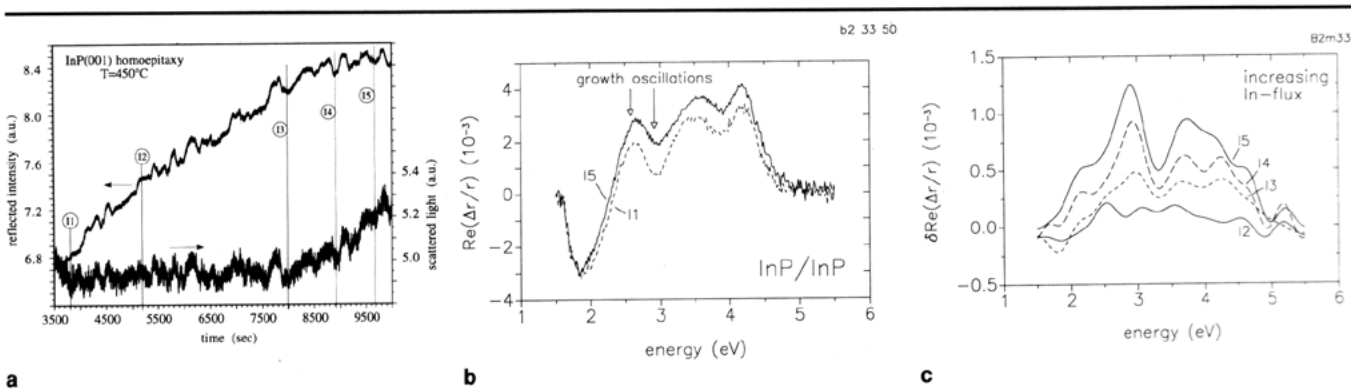

Fig. 8. (a) Time evolution of the PRS signal and diffuse scattering light intensity for homoepitaxial InP film growth at 450°C under PCBE conditions with a 3 s cycle sequence time, (b) RDS spectra in the early stage of growth (I1) and after prolonged growth under high TMIn:TBP ratio (I5), and (c) relative changes in the anisotropy observed in the RDS-spectra at selected points I2 through I5 as marked in Fig. 8 (a) (with respect to I1). The difference spectra are filtered to enhance the structures. Additional features seen e.g. around 2.2 eV are numerical artifacts.

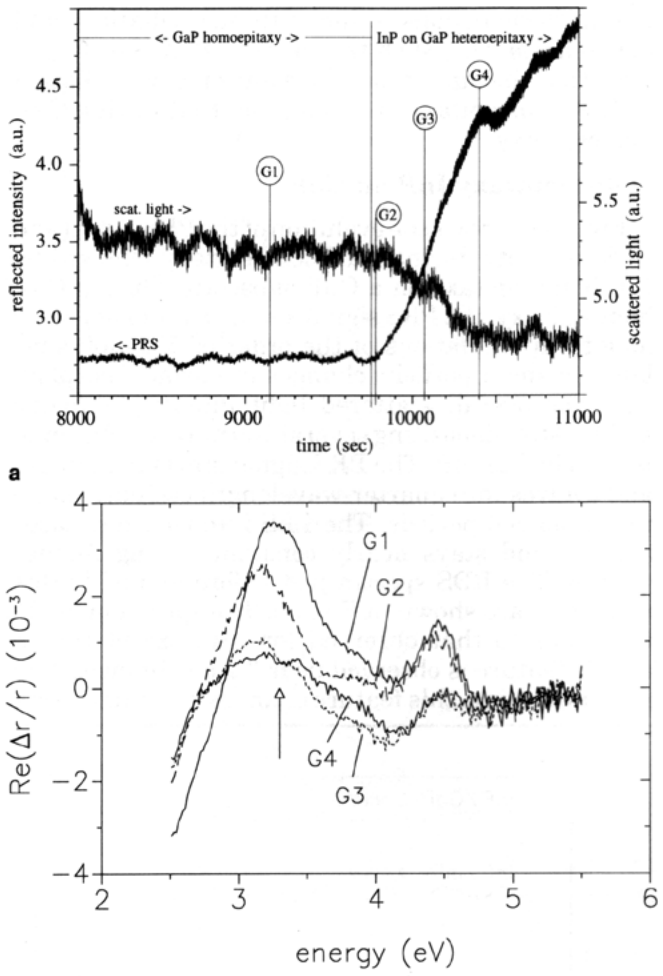

Fig. 9. (a) P-polarized reflectance signal (upper curve) and scattered light intensity (lower curve) for heteroepitaxial InP layer grown on GaP(001) at 450°C with a 3 s cycle sequence time, and (b) time evolution of the RDS-signal at selected points as marked in Fig. 8 (a): G1: during GaP homoepitaxy, G2 through G4 during InP film growth.

and shifts toward lower energies, as expected for InP because the spectral position for InP is near 2.6 eV. With increasing coverage all features become weaker with that near 3 eV broadening significantly. An additional small feature at 3.2 eV is near in energy to that observed for as-cleaned InP surfaces covered by a very thin oxide. Since this feature is not observed during InP homoepitaxy, it is likely to be due to strain in the substrate surface region induced by the oxide film. Therefore, we interpret this feature during the heteroepitaxy as a result of the (compressive) strain in the InP due to the high lattice mismatch between InP and GaP. Another explanation is the linear optical effect observed earlier in doped GaAs.[22]

SUMMARY AND CONCLUSION

We have applied PRS, RDS, and LLS to monitor low-temperature homoepitaxial growth of GaP and InP and heteroepitaxial growth on Si during pulsed chemical beam epitaxy. These methods show that alternatively supplying V-III precursors results in a periodic change of the chemical composition of the surface, which appears either as a periodic oscillation of the anisotropy as measured by RDS or as oscillations in PRS. In the case of heteroepitaxial growth, PRS also exhibits a quarter-wavelength oscillating component. The long-term variations of the PRS and LLS signals are interpreted as periodic changes of surface topography.

We have also investigated surface modifications with various III-V precursor ratios. For InP growth, the surface roughens for a III-V precursor ratio less than 60:1, which is slightly higher than that found for GaP.

ACKNOWLEDGMENTS

This work has been supported by the NFS grant DMR 9202210, the Office of Naval Research under Contract ONR-00014-1-0255 and by the Alexander von Humboldt Foundation.

REFERENCES

1. A.Y. Cho, J. *Appl. Phys.* 42, 2074 (1971).
2. D.E. Aspnes, R. Bhat, E. Colas, V.G. Keramidas, M.A. Koza and A.A. Studna, *J. Vac. Sci. & Technol. A* 7 (3), 711 (1989).
3. H. Zama, K. Sakai and S. Oda, *Jpn. J. Appl. Phys.* Part 2, 31 (9A), L1243 (1992).
4. N. Kobayashi, T. Makimoto, Y. Yamauchi and Y. Horikoshi, *J. Cryst. Growth* 107 (1-4), 62 (1991).
5. T. Makimoto, Y. Yamauchi, N. Kobayashi and Y. Horikoshi, *Jpn. J. Appl. Phys.* 29 (2), L207 (1990).
6. K.A. Bertness, C. Kramer, J.M. Olson and J. Moreland, *J. Electron. Mater.* 23 (2) 195 (1994).
7. J.V. Armstrong, T. Farrell, T.B. Joyce, P. Kightley, T.J. Bullough and P.J. Goodhew, *J. Cryst. Growth* 120, 84 (1992).
8. K.P. Killeen and W.G. Breiland, *J. Electron. Mater.* 23 (2), 179 (1993).
9. H. Grothe and F.G. Boebel, *J. Cryst. Growth* 127, 1010 (1993).
10. D.E. Aspnes, W.E. Quinn, M.C. Tamargo, M.A.A. Pudensi, S.A. Schwarz, M.J.S.P. Brasil, R.E. Nahory and S. Gregory, *Appl. Phys. Lett.* 60 (10), 1244 (1992).
11. N. Dietz, A.E. Miller, J.T. Kelliher, D. Venables and K. J. Bachmann, *Proc. Eighth Int. Conf. on Molecular Beam Epitaxy,* Osaka, Japan, 29 Aug. 1994, *J. Cryst. Growth* 150, 691 (1995).
12. N. Dietz, A.E. Miller and K.J. Bachmann, *J. Vac. Sci. Technol. A* 13 (1), 153 (1995).
13. K.J. Bachmann, N. Dietz, A.E. Miller, D. Venables and J.T. Kelliher, *J. Vac. Sci. Technol. A* 13 (3) 696 (1995).
14. A.E. Miller, J.T. Kelliher, N. Dietz and K.J. Bachmann, *Mater. Res. Soc. Symp. Proc.* 355, (Pittsburgh, PA: Mater. Res. Soc., 1995), p.197.
15. D.E. Aspnes, J.P. Harbison, A.A. Studna, L.T. Florez and M.K. Kelly, *J. Vac. Sci. & Technol. A* 6 (3), 1327 (1988).
16. A.A. Studna, D.E. Aspnes, L.T. Florez, B.J. Wilkens and R.E. Ryan, *J. Vac. Sci. & Technol. A* 7 (6) 3291 (1989).
17. J.T. Kelliher, J. Thornton, N. Dietz, G. Lucovsky and K.J. Bachmann, *Mat. Sci. & Eng. B* 22, 97 (1993).
18. M. Ebert, U. Rossow, L. Mantese, K. Ploska, W. Richter and D.E. Aspnes, *Proc. of the ICFSI-5,* Princeton June 1995, to be published in *Appl. Surf. Sci.* (1995).
19. T. Yasuda, L. Mantese, U. Rossow and D.E. Aspnes, *Phys. Rev. Lett.* in print (1995).
20. L. Mantese, U. Rossow, T. Tasuda and D.E. Aspnes, *Proc. of the ICFSI-5,* Princeton June 1995, to be published in *Appl. Surf. Sci.* (1995).
21. P. Kurpas, J. Jonsson, W. Richter, D. Gutsche, M. Pristovsek and M. Zorn, *J. Cryst. Growth* 145, 36 (1994).
22. S.A. Acosta-Ortiz and A. Lastra-Matrinez, *Sol. State Commun.* 64, 809 (1987).